Journal Pre-proof

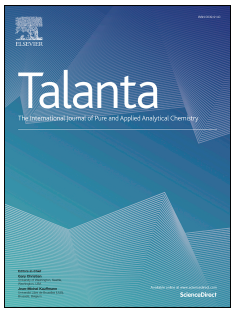

Electrochemical aptasensor for NS1 detection: towards a fast Dengue biosensor

Bassam Bachour Junior, Marina Ribeiro Batistuti, Aline Sanches Pereira, Elisa Maria de Sousa Russo, Marcelo Mulato

PII: S0039-9140(21)00448-3

DOI: https://doi.org/10.1016/j.talanta.2021.122527

Reference: TAL 122527

To appear in: *Talanta*

Received Date: 21 January 2021

Revised Date: 10 May 2021

Accepted Date: 12 May 2021

Please cite this article as: B. Bachour Junior, M.R. Batistuti, A.S. Pereira, E. Maria de Sousa Russo, M. Mulato, Electrochemical aptasensor for NS1 detection: towards a fast Dengue biosensor, *Talanta*, https://doi.org/10.1016/j.talanta.2021.122527.

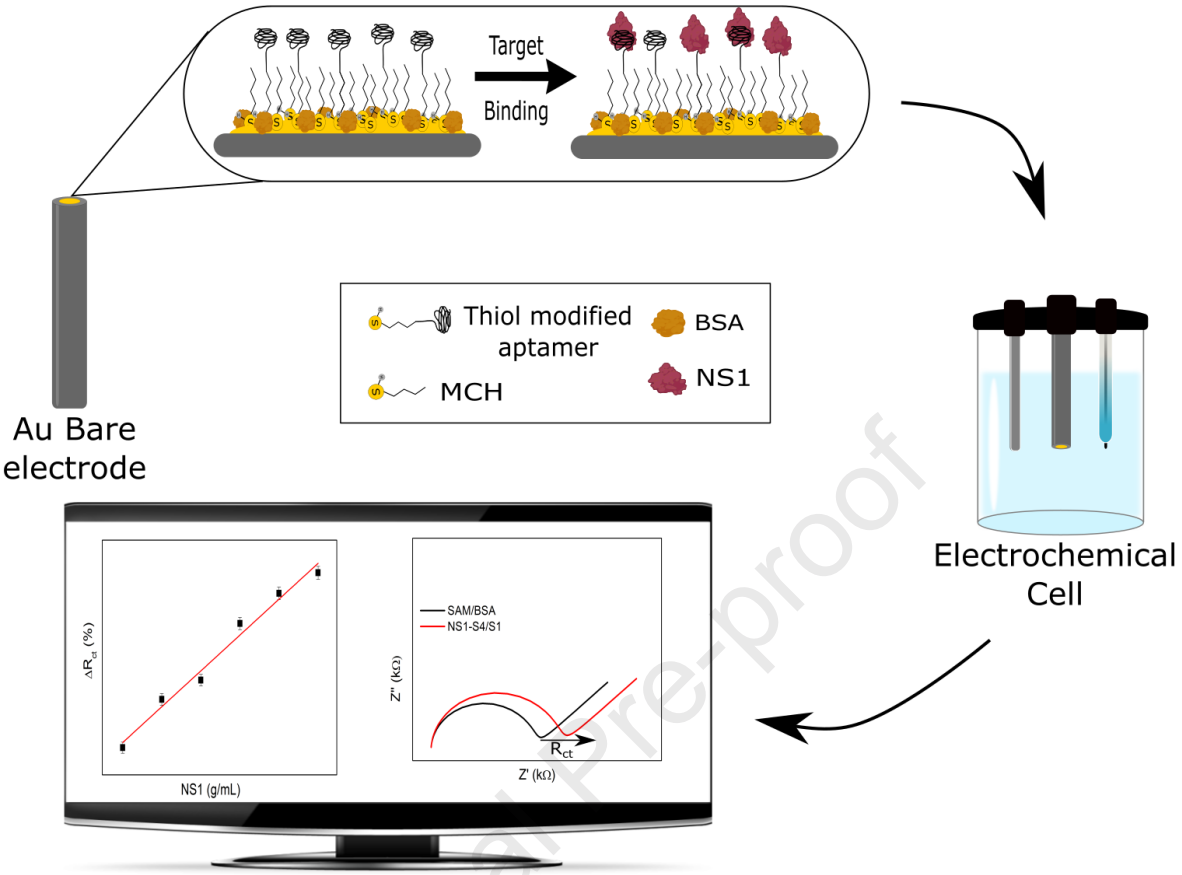

Electrochemical aptasensor for NS1 detection: towards a fast Dengue biosensor

Bassam Bachour Junior[1], Marina Ribeiro Batistuti*[1], Aline Sanches Pereira[2], Elisa Maria de Sousa Russo[2] and Marcelo Mulato[1]

[1] Department of Physics, Faculty of Philosophy, Sciences and Letters at Ribeirão Preto, University of São Paulo, Brazil.

[2] Department of Clinical Analyses, Toxicology and Food Science, School of Pharmaceutical Sciences of Ribeirão Preto, University of São Paulo, Brazil

[*]*Corresponding Author:* Marina R. Batistuti (marbatistuti@usp.br)

Abstract

Dengue is one of the most commonly neglected tropical diseases transmitted by *Aedes aegypti* infected with Dengue virus. This virus belongs to the gender *Flavivirus* and produces a non-structural protein 1 (NS1), which is an important biomarker found at high levels in blood in early disease stage. Therefore, this study focused on the development of an electrochemical biosensor for NS1 detection using DNA aptamers. Gold electrodes were co-immobilized with specific aptamers and 6-mercapto-1-hexanol (MCH) to obtain a self-assembled monolayer. The molar ratio between aptamers and MCH was optimized and the platform characterized by electrochemical impedance spectroscopy and atomic force microscopy. Bovine serum albumin was added in NS1 solution to stabilize it and block the surface to avoid non-specific interactions. The biosensor performance was tested with NS1 protein serotype 4 (in phosphate saline buffer and human serum) and with a solution of serotype 1 in human serum. The results showed a sensitivity of 2.9 %, 2.7 % and 1.7 % per decade, respectively, and low limit of detection (0.05, 0.022 and 0.025 ng/mL). The platform was also tested with Envelope protein as negative control. Furthermore, the aptamer sensor was able to detect NS1 in clinical range and it is a promising candidate for a new class for miniaturized point-of-care device for different Dengue serotypes.

Keywords: Aptamer; Dengue; NS1; Biosensor; Impedimetric.

Introduction

Dengue is the most common non-contagious infectious disease in the world, mainly in tropical and subtropical regions. The disease is caused by the bite of infected mosquito with Dengue virus [1]. This virus belongs to gender *Flavivirus*, *Flaviviridae* virus family (DENV) and present five different serotypes (DENV - 1, DENV - 2, DENV - 3, DENV – 4 and DENV - 5), which makes it difficult to create an unique vaccine [2,3]. This disease exhibits symptoms similar to a normal flu on the first infection [4]. In the second infection, the symptoms can be more aggressive, and in some cases, lead to death [5,6]. In Brazil, Dengue has evolved from an endemic to hyperendemic disease [7], and only in 2019 over 1.4 million cases and 500 deaths occurred [8].

The virus encodes three structural proteins (capsid, membrane and envelope glycoprotein). From these proteins, the envelope glycoprotein, or E protein, has an important role been associated with receptor binding, hemagglutination of erythrocytes, production of neutralizing antibodies and immune response [4].

Others seven non-structural proteins (NS1, NS2A, NS2B, NS3, NS4A, NS4B and NS5) are also encoded by the virus, but only NS1 is continuously secreted in blood by the infected host cell [9], mainly in the first days of infection up to 9 days after the onset [10]. NS1 is a glycoprotein with approximately 46-50 kDa, highly conserved among the four DENV serotypes [11,12]. Alcon *et al.* reported NS1 levels on human serum as 0.04 to 2 μg/ml on the first and 0.01 to 2 μg/ml on the second infection [13]. These characteristics made NS1 an important biomarker for Dengue.

The standard technique to detect Dengue NS1 for diagnostic purposes is enzyme-linked immunosorbent assay (ELISA). This technique as well as the chemiluminescence needs high-cost equipment. ELISA technique recognizes the binding event of one target (protein) and antibody (IgG, IgM) using an optical sensor. This technique can detect dengue infections up to 9 days after the onset of disease [14]. However, it is not a portable system [15] and needs high expertise to manipulate it [16]. To solve this problem, many researchers have investigated the biosensors as an alternative to detect dengue biomarkers, such as NS, looking for techniques with low cost, high sensitivity and simple fabrication [17].

Aptamers are one of the options. They consist in a small single-stranded oligonucleotides (DNA or RNA) sequence that is able to bind targets with high affinity, specificity and used analogs of antibodies. These targets vary from simple molecules to large and complex proteins, or even the hole cell. Aptamers are developed by SELEX (systematic evolution of ligands by exponential enrichment) [18,19], an *in vitro* method that is easier and cheaper than the methods used for antibodies production [20,21]. These three-dimensional structures present other significant advantages over the antibodies, once they can be used in Western blotting and ELISA protocols with high sensitivity [22–25], purify target proteins [26,27], and are not toxic or immunogenic [28].

Aptamers have been successfully used as recognizing elements for biosensing over the last years [29,30]. In this case, the surface density is higher once they are smaller than antibodies [31,32], increasing the response. Aptamers also present high stability, are easier to modify and have lower cost [33,34]. Among the biosensors, electrochemical transducers are the most developed class with relative simplicity, low-cost, miniaturization and easy to use portable devices [34]. Electrochemical impedance spectroscopy (EIS) is widely used to study the changes on electrode surface, including the interaction between receptors and analyte by a small perturbation in frequency domain range with a fixed potential [35].

In 2017, Lee and Zeng published an article describing the development of different DNA aptamers for NS1 protein from Zika and Dengue [16]. The sequences were tested over different NS1 concentrations from Zika and 10 nM NS1 from DENV 1, 2, 3 and 4. The results show a successful ELISA-based assay with highly specific and sensitive detection of Zika NS1 antigen using an aptamer/aptamer pair and using a hybrid aptamer/antibody pair.

In the literature, there are really few articles focused on Dengue study through aptamers. Therefore, due to all advantages on using single strand oligonucleotides, the novelty proposed here is the development and characterization of a fast aptasensor platform for Dengue detection using as recognizing element one of the aptamer sequence developed by Lee and Zeng. The platform was based on a self-assembled monolayer (SAM) co-immobilized with aptamers and MCH. Biosensor performance was tested with NS1 protein serotype 1 and 4 in PBS and human serum using EIS.

Experimental

Materials

All chemicals, 6-Mercapto-1-hexanol ($HS(CH_2)_6OH$) and DNA aptamer thiol modified sequence (5' - $HS(CH_2)_6$ – TTTTT – ACTAGGTTGCAGGGGACTGCTCGGGATTGCGGAT CAACCTAGTTGCTTCTCTCGTATGAT – 3') [16] were purchased from Sigma-Aldrich. The NS1 protein serotype 4 (NS1-S4) was purchased from Abcam (ab181957). All aqueous solutions were prepared using 18.2 MΩ cm ultra-pure water (Merck Milipore Direct-Q 5UV) with Biopak Polisher filter (Merck Milipore, CDUFB-001) to remove nuclease.

Protein expression

NS1 serotype 1 (NS1-S1) was expressed using a synthetic full-length NS1 gene of dengue virus serotype 1 cloned into pET28a vector to construct plasmid pET28a_DENVNS1. The recombinant plasmid was used to transform *Escherichia coli* strain Rosetta (DE3) and the protein expression was induced with 1.0 mM isopropyl β-D-1-thiogalactopryanoside (IPTG) in mid-log phase growth (OD_{600} = 0.4 - 0.6) for 4h at 37 ℃. The protein was expressed in inclusion bodies which were solubilized under denaturing conditions and the recovered protein was purified by nickel affinity chromatography. The size of the expressed protein was approximately 45 kDa and identified by Western Blotting using anti-His tag antibody. In addition, NS1-S1 was recognized in a commercial Immuno chromatographic strip for detection of dengue NS1 antigens (Wama diagnostic). More details about the proteins expressions are presented in Supplementary material.

Measurement and apparatus

The potentiostat (Metrohm/Autolab PGSTAT302) was used with a three-electrode cell configuration: Ag/AgCl (FACTE) as reference electrode, platinum wire (Metrohm) as counter electrode and gold electrodes with 2 mm diameter (Metrohm) as working electrodes. Biosensor development was characterized via atomic force microscopy (AFM) using a Shimadzu SPM-9600 Scanning Probe Microscopy (Shimadzu Corporation, Japan). Scanning was performed in air at 25 °C.

Electrode preparation and functionalization

DNA aptamer was incubated at 94 °C in water bath for 10 min followed by dilution in SELEX solution (20 mM Tris pH 7.5 + 150 mM NaCl +1 mM $MgCl_2$ +2.7 mM KCl + 0.005% $C_{12}E_8$) at room temperature (24 ºC) for 40 min to achieve the folded structure [16]. This solution was mixed with MCH (10% ethanol) in different molar ratios. The ratios are presented as [Apt / (total thiol)]. Total thiol corresponds to the sum of aptamer and MCH in solution.

Working electrodes were desorbed using cyclic voltammetry in NaOH (0.5 M) from - 2.0 to - 0.8 mV (vs. Ag/AgCl) for 30 cycles. Then, they were polished with different alumina size (1 and 0.3 μm, sequentially), followed by sonication in water for 5 min between each polish. After this procedure, the electrodes were electrochemically cleaned in H_2SO_4 (0.5 M) by scanning potential from - 0.5 to 1.1 V (vs. Ag/AgCl) for 25 cycles [35]. Gold clean electrodes were dried with N_2 and co-immobilized using 150 μL SELEX solution with aptamer and MCH for 18 h in a humidity chamber at 4 ºC.

After surface modification, the electrodes were rinsed with three solutions (200 mM phosphate buffer (PB); 10 mM PB + 100 mM ethylenediaminetetraacetic acid (EDTA); 10 mM PB) for 5 min each. To prevent non-specific interaction and ensure the total thiol coverage, electrodes were backfilled with 150 μL of MCH (10% ethanol) for 1 h. Afterwards, electrodes were rinsed with ultra-pure water and immediately immersed in 400 μl of PBS (137 mM NaCl + 2.7 mM KCl + 1 mM Na_2HPO_4 + 0.18 mM KH_2PO_4, pH 7.4) for 2 h to stabilize the platform [35]. Finally, the electrodes were blocked with 150 μL of BSA (0.1 %) in PBS or serum for 30 min. Figure 1(a) shows an illustration of co-immobilization solution preparation and SAM architecture.

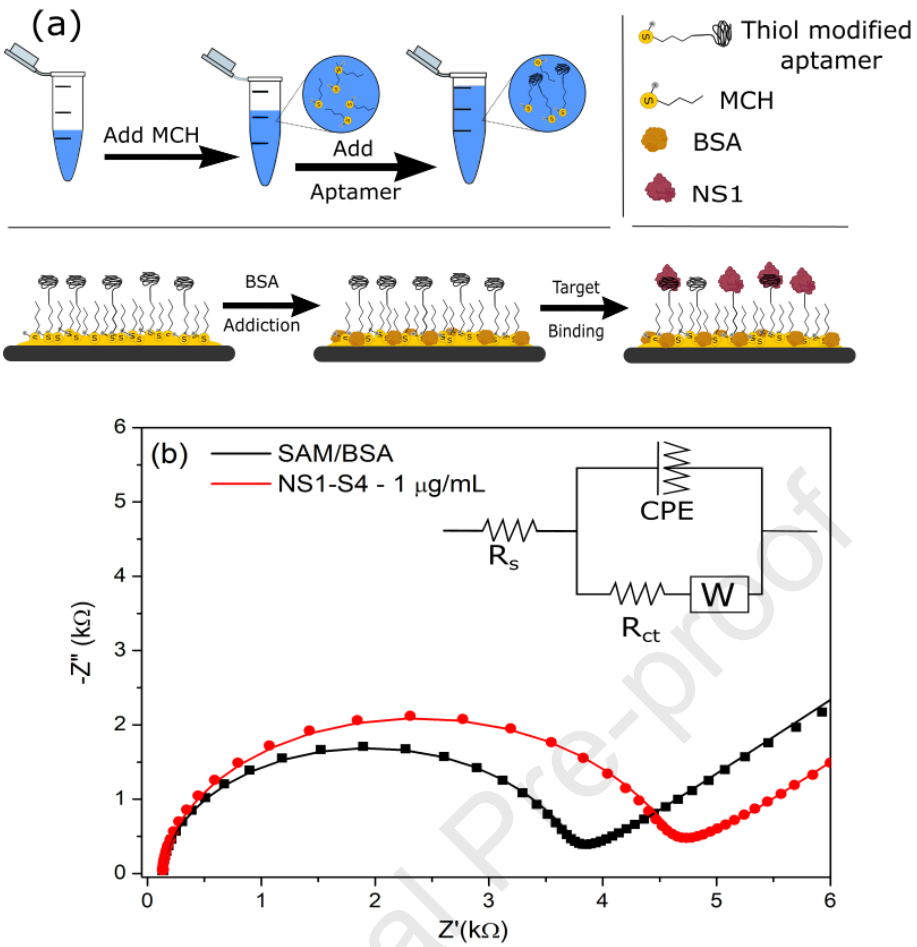

Figure 1. In (a) an illustration of co-immobilization solution preparation and surface architecture on top of gold electrode after BSA blocking and NS1 binding. In (b) Nyquist diagram using electrochemical impedance spectroscopy from SAM blocked with BSA (square) and binding with 1 µg/mL NS1-S4 (circle). The inset in (b) shows the Randle's equivalent circuit adopted as model to fit the data.

Electrode characterization

The EIS measurements were obtained in the frequency range from 100 kHz to 100 mHz with a 10 mV a.c. voltage superimposed on a d.c. bias of open circuit potential (OCP) configuration (approximately - 0.23 mV) using 2.5 mM $C_6FeK_4N_6$ + 2.5 mM $C_6FeK_3N_6$ (1:1) in PBS. All data was fitted using Randle's equivalent circuit (Fig. 1(b) inset). The charge transfer resistance (R_{ct}) represents the electrical signal for SAM and protein binding; Warburg diffusion element (Z_w) corresponds to the diffusion process in the solution; Constant phase element (CPE) corresponds to non-pure capacitor to represent the electrode inhomogeneity and

surface roughness, and R_s represents the electrolytic solution resistance [36,37]. Figure S.1 (Supplementary material) describes the equivalent circuit with more details.

Data Analysis

The data was fitted using Autolab software (Nova 2.1) and the equivalent circuit adjustments were evaluated through qui-square test with values under 10^{-2}. Each electrode data were normalized by surface roughness using the reduction peak area divided by the reduction charge per microscopic area (390 ± 10 μC/cm²) [38, 39]. All electrodes measures were repeated three times and the standard average was obtained with standard deviation error according to equation S.2 and S.3 (Supplementary material) to guarantee the repeatability. Each experiment was repeated at least two times to evaluate the reproducibility.

Results and Discussion

Self-assembled monolayer

Monolayer organization allows the development of a stable biorecognition surface with a low interference of non-specific targets. In this case, electrodes were incubated with thiolate DNA aptamer solution and MCH. The thiol termination has a high affinity and makes a strong covalent binding on the gold surface. This spontaneous organization form a compact monomolecular film with a weak electrostatic attraction between alkyl chains that helps to stabilize and orientate the molecules [38].

Characterization of DNA aptasensor

AFM images of different modifications on gold electrode are shown in Figure 2: (a) corresponds to clean electrode with 113 nm highest peak and (b) corresponds to MCH modification (41 nm) using a 1.00 x 1.00 μm resolution. This difference in the surface height evidences the smoothness on gold electrode surface after MCH immobilization. Figure 2(c) shows the SAM architecture with DNA aptamer co-immobilized with MCH, where the surface height increases due to the aptamer size to 43 nm compared with (b). The SAM blocked with BSA is shown in Figure 2(d) with a surface height increased to 71 nm after 1 μg/mL NS1-S4 protein interaction with the aptamer.

One important parameter to evaluate AFM images is the average surface roughness (R_a) [40,41]. Clean bare electrodes presented 9.31 nm and MCH 3.99 nm. For SAM modification, the R_a factor exhibited 4.90 nm and for the NS1 interaction 6.34 nm. These values corroborate that the aptamer immobilization increases the surface roughness compared to the MCH

immobilization due to its size and the NS1 protein interaction can be verified once it also increases the surface height.

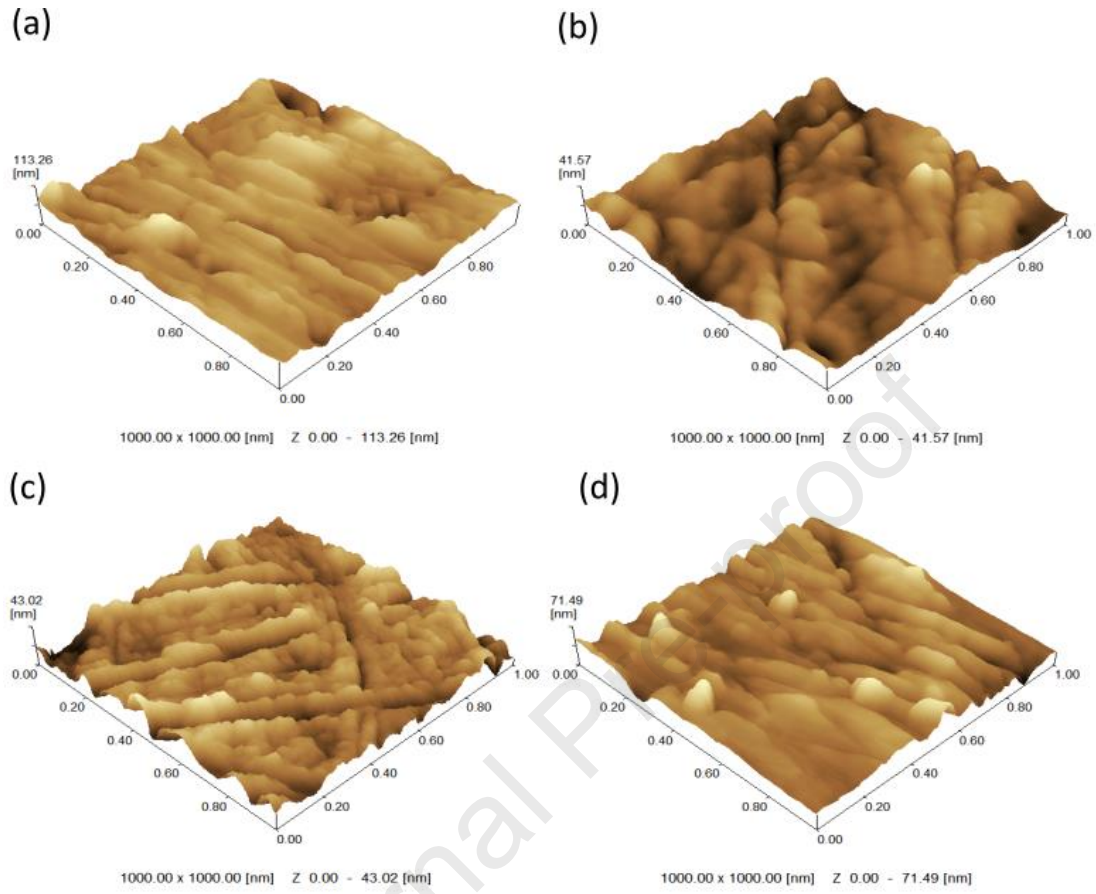

Figure 2. AFM images: (a) corresponds to clean bare electrode with 113 nm surface height, (b) the surface height decreases due to MCH modification to 41 nm. The modified SAM increased the surface roughness due to the aptamer presence to 43 nm in (c) and (d) shows the increase when the SAM blocked with BSA interacts with 1 µg/mL NS1-S4 to 71 nm. All the AFM images were analyzed in 1 x 1 µm resolution.

NS1 protein stability and surface density for aptamer/MCH

EIS is a powerful technique to characterize and quantify the surface interactions by measurements of charge transfer resistance (R_{ct}). This variation (ΔR_{ct}) evidences the binding between the aptamer and NS1 (Equation S.1) [ΔR_{ct} (%) = (R_{ct}(target)–R_{ct}(blanck)) / R_{ct}(blanck) x 100 %]. The platform stability was verified by repeating EIS measurements every 30 min, at least 3 times, before target interaction.

The protein was tested with and without BSA due to its structure stability [42]. Figure 3(a) shows in solid squares this interaction, where ΔR_{ct} (%) = 5.26 + 0.39log C_{NS1} (C_{NS1} in the

concentration of NS1 in g/mL). This sensor exhibits a sensitivity of 0.39 % per decade (log C_{NS1}) with a correlation coefficient of 0.27. The low ΔR_{ct} signal variation (3 %) in high value of NS1 concentration (1 µg/mL) indicates any process that prevent or hinders the NS1 binding to the surface. To increase this signal, BSA (0.1 %) was diluted in the NS1 buffer solution to interact with cysteine residues [16]. The open squares on Figure 3(a) show that the signal improved to 10%, with a sensitivity of 1.65 % per decade (log C_{NS1}) and correlation coefficient of 0.94.

Keighleys et al. described the SAM performance optimization though surface density [35]. Thus, the platform was optimized with different molar ratios between aptamer and MCH (1:25, 1:50, 1:100, 1:150 and 1:200) and its interaction with 100 pg/mL NS1 using buffer solution (PBS + BSA 0.1%, pH 7.4). The results presented in Figure 3(b) and in Table S.1 in the Supplementary material confirm that surface density is an important parameter [35]. MCH concentration affects SAM organization and helps to reduce electrostatic interaction between DNA negative charge [43,44]. In this case, 1:150 ratio provided the optimized signal (7.3 %) and was used for further experiments.

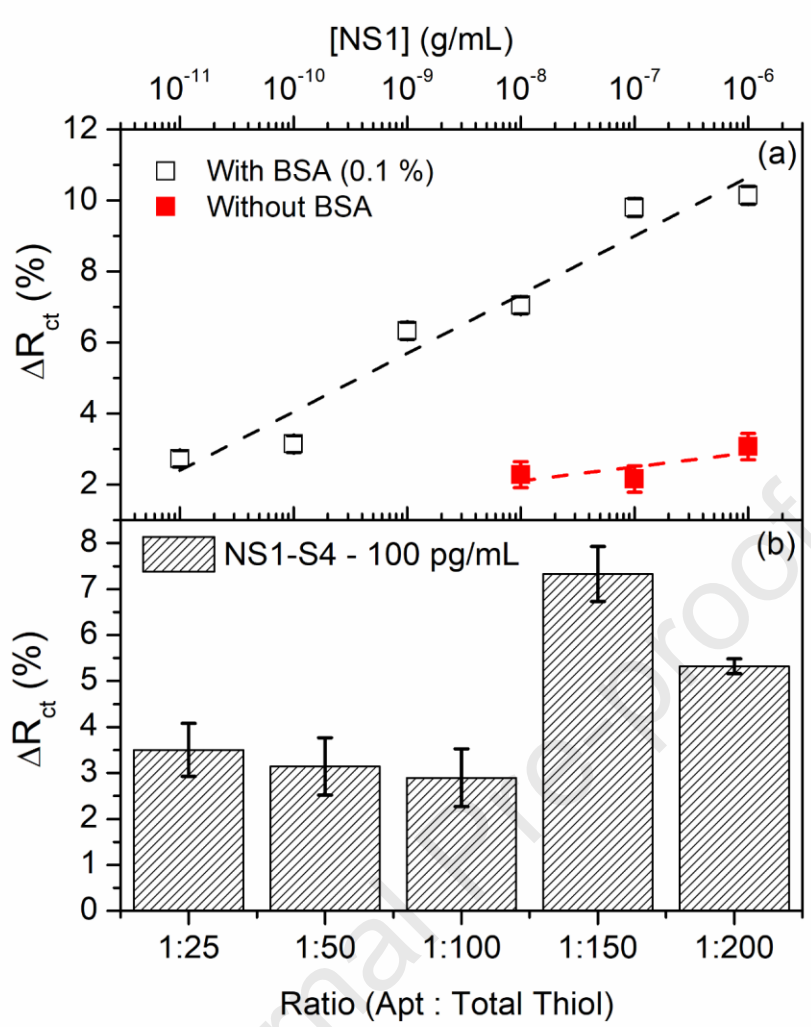

Figure 3. Change in charge transfer resistance (ΔR_{ct}). (a) stability test for NS1-S4 with BSA (0.1 %) in PBS (pH 7.4) solution (open square) and NS1-S4 without BSA in solution (solid square); (b) aptamer/MCH molar fraction (apt : total thiol) with 100 pg/mL NS1-S4 in PBS (pH 7.4) + BSA (0.1%) solution. Error bars show the standard deviation for at least three measurements from different electrodes.

Analytical Curve

Gold electrodes modified with SAM in the optimized ratio were tested from 10 pg to 1 µg/mL NS1 – S4 (Figure 4). The electrodes were first blocked with BSA (0.1%) in PBS (pH 7.4) and the signal was used as a baseline to all NS1 interactions. After that, the electrodes were incubated with 100 µL of NS1 solutions in different concentrations for 30 min and washed with PBS (pH 7.4) to remove unbound NS1 molecules. Figure S.2, S.3 and S.4 in Supplementary material exhibits the Nyquist diagram for each NS1 dilution in different solution. The solid squares in Figure 4 show the ΔR_{ct} increase for each NS1 concentration in PBS + BSA (0.1 %)

in a linear range (10 pg to 1 µg/mL). Figure S.5 shows the analytical curve for all buffer and serum dilution. The open squares exhibit signals for NS1 incubation in undiluted serum with a linear range from 10 pg to 100 ng/mL and a plateau at 100 ng/mL (Table S.2 indicates the analytical results in Supplementary material). This plateau indicates the surface saturation due to the high amount of other proteins and molecular agglomerates on it. The limit of detection (LoD) was obtained by LoD = 3.3 x σ/b, σ represents standard deviation and b represents the slope of analytical curve [45]. For buffer solution, the LoD correspond to 0.05 ng/mL with sensitivity of 2.9 % per decade. In undiluted serum, the limit reached 0.02 ng/mL and the sensitivity of 2.7 % per decade. Both results show a good sensitivity comparing to other techniques reported in the literature. Table 1 presents a comparison between the results from this study and the state-of-art for NS1 detection over the last 5 years

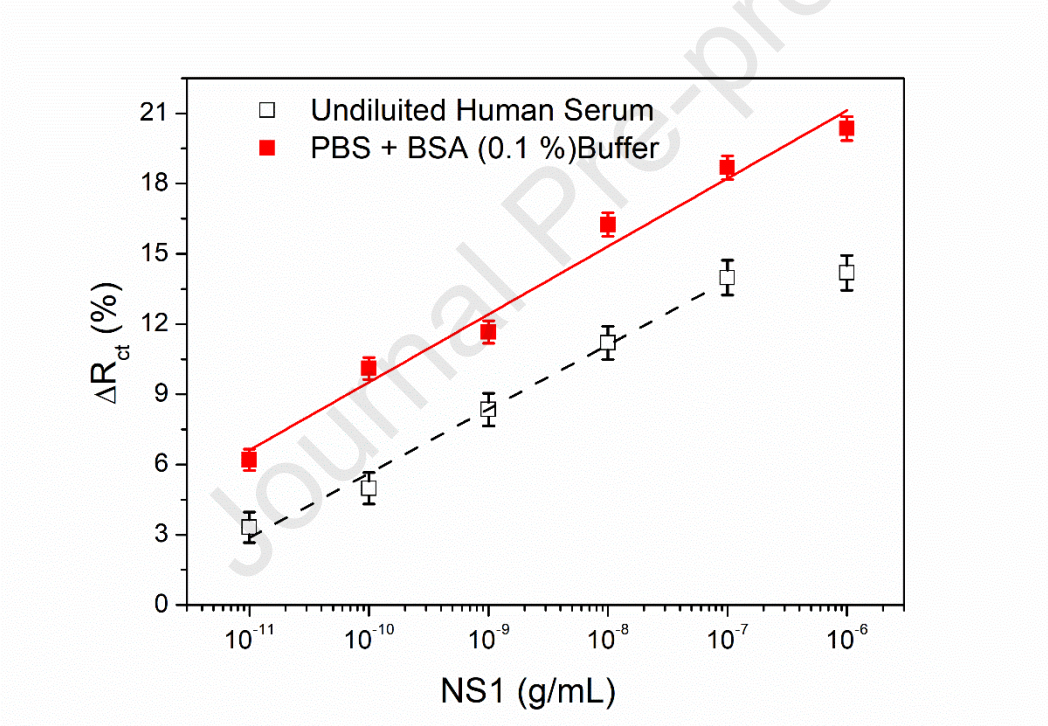

Figure 4. Analytical curve for NS1-S4 diluted in buffer (solid square) and commercial undiluted human serum (open square). Error bars show the standard deviation from at least three individual electrodes.

Selectivity

Lee and Zeng demonstrated the ability of this DNA aptamer to detect more than one serotype from NS1 [16]. To confirm this, two NS1 serotypes (S4 and S1) were tested over different concentrations. Serotype 4 exhibits que highest binding to the aptamer [16] and serotype 1 is the most common form [46]. Figure 5(a) compares the analytical curve in

undiluted human serum for NS1-S4 and NS1-S1. The results from NS1-S4 were discussed in the last section. NS1-S1 was expressed, purified and lyophilized. Before the experiment, the protein was suspended and interacted with the platform with a linear range from 10 pg/mL to 1µg/mL with 0.025 ng/mL as LoD and sensitivity of 1.7 % per decade.

The negative control was performed with E protein, an envelope protein also expressed during Dengue infection, comparing to NS1-S4 and NS1-S1 in undiluted human serum. In Figure 5(b) it is possible to observe that serotype 1 exhibited a change in charge transfer resistance increase over 9 %, close to 8 % from serotype 4, comparing to envelope protein, with negative change in R_{ct}.

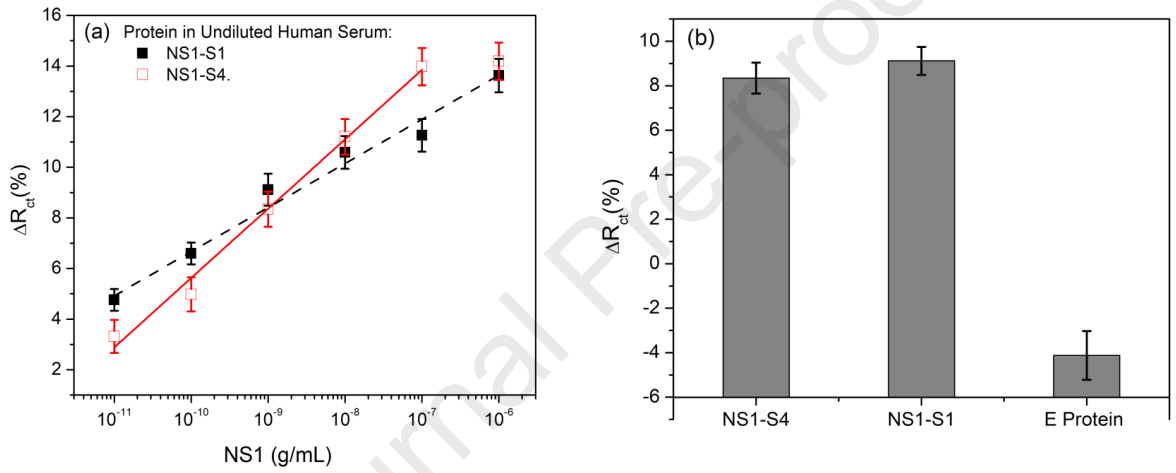

Figure 5. Selectivity control. In (a) the analytical curve comparing the biosensor performance for NS1-S1 and S4 in undiluted human serum. Error bars show the standard deviation from at least three individual electrodes. In (b) change in charge transfer resistance (ΔR_{ct}) for 1 ng/mL of different Dengue proteins in undiluted human serum: NS1-S4, NS1-S1 and Envelope protein (E Protein).

The electrochemical aptasensor platform presented a good selectivity over different Dengue proteins, with the ability to recognize the two tested serotypes with a linear range over the clinical range and low limit of detection, emerging as a future device for clinical applications.

Table 1. Comparison between the present study and state-of-art technologies over the last 5 years.

Bioreceptor	Technique	LoD (ng/mL)	Sensitivity	Linear Range	Solution	Serotype	Reference
Peptides	Impedimetric	1500	[]*	0.025 to 12.5 μg/mL	Buffer	2	[47]
Antibody	Potentiometric	[]*	-4.52 per log ng/mL	10^{-6} to 10^{-3} mg/mL	Artificial Saliva	2	[48]
Antibody	Capacitive	0.34	4.5 % per decade	1 to 5000 ng/mL	Buffer	[]	[49]
Antibody	Capacitive	1.2	6.7% per decade	5 to 1000 ng/mL	Diluted serum (1:5)	[]	[49]
Antibody	Optical	15	[]*	15 to 500 ng/mL	Buffer	2	[50]
Antibody	Impedimetric	30	10.4 % per decade	10 to 1000 ng/mL	Undiluted serum	2	[51,52]
Antibody	Capacitive	0.5	22 % per decade	5 to 1000 ng/mL	Undiluted serum	2	[51]
Antibody	Impedimetric	0.5	[]*	1 to 25 ng/mL	Buffer	2	[53]
Antibody	Amperometric	12	85.6 μA/mM	40 to 2000 ng/mL	Buffer	[]	[54]
Aptamer	**Impedimetric**	**0.05**	**2.9 % per decade**	**0.01 to 1000 ng/mL**	**Buffer**	**4**	**This work**
Aptamer	**Impedimetric**	**0.022**	**2.7 % per decade**	**0.01 to 100 ng/mL**	**Undiluted serum**	**4**	**This work**
Aptamer	**Impedimetric**	**0.025**	**1.7 % per decade**	**0.01 to 1000 ng/mL**	**Undiluted serum**	**1**	**This work**

[]*: data not available.

Conclusion

We developed a new platform for fast NS1 detection using specific DNA aptamer using electrochemical technique. The electrodes were successfully characterized by AFM to confirm surface modification and protein binding through changes in surface roughness. NS1 protein showed a different behavior in the presence or absence of bovine serum albumin protein. The aptamer-based sensor showed a good sensitivity to detect NS1 protein in a large dynamic range in buffer and in undiluted human serum, fast response time, low cost and a high degree of selectivity against other Dengue protein. In addition, the biosensor was capable to detect serotypes 1 and 4 in clinical range for first (40-2000 ng/mL) and second (10-2000 ng/mL) infection being a promising tool for miniaturization and point-of-care device.

Acknowledgements

B.B. Jr was financed by the Coordenação de Aperfeiçoamento de Pessoal de Nível Superior - Brasil (CAPES- Finance Code 001). M.R.B. was funded by FAPESP (process number 2013/26133-7). A.S.P. was funded by the Coordenação de Aperfeiçoamento de Pessoal de

Nível Superior - Brasil (CAPES - Finance Code 001). M.M. was funded by FAPESP (process number 2017/24201-6) and CNPq (308713/2018-4).

Author Contributions

B.B.Jr. performed the experiments and analyzed data. M.R.B. design and helped with the experiments. A.S.P expressed the NS1 protein serotype 1 and E protein. The paper was written by B.B.J. and M.R.B. with contributions by A.S.P and revised by M.M. and E.M.S.R. The work was supervised by M.M.

Reference

[1] L.P. de G. Cavalcanti, A.R.R. Freitas, P. Brasil, R.V. da Cunha, Surveillance of deaths caused by arboviruses in Brazil: from dengue to chikungunya, Mem. Inst. Oswaldo Cruz. 112 (2017) 583–585. https://doi.org/10.1590/0074-02760160537.

[2] S. Bhatt, P.W. Gething, O.J. Brady, J.P. Messina, A.W. Farlow, C.L. Moyes, J.M. Drake, J.S. Brownstein, A.G. Hoen, O. Sankoh, M.F. Myers, D.B. George, T. Jaenisch, G.R.W. Wint, C.P. Simmons, T.W. Scott, J.J. Farrar, S.I. Hay, The global distribution and burden of dengue, Nature. 496 (2013) 504–507. https://doi.org/10.1038/nature12060.

[3] M.S. Mustafa, V. Rasotgi, S. Jain, V. Gupta, Discovery of fifth serotype of dengue virus (DENV-5): A new public health dilemma in dengue control, Med. J. Armed Forces India. 71 (2015) 67–70. https://doi.org/10.1016/j.mjafi.2014.09.011.

[4] M.G. Guzman, S.B. Halstead, H. Artsob, P. Buchy, J. Farrar, D.J. Gubler, E. Hunsperger, A. Kroeger, H.S. Margolis, E. Martínez, M.B. Nathan, J.L. Pelegrino, C. Simmons, S. Yoksan, R.W. Peeling, Dengue: a continuing global threat, Nat. Rev. Microbiol. 8 (2010) S7–S16. https://doi.org/10.1038/nrmicro2460.

[5] P. Gurugama, P. Garg, J. Perera, A. Wijewickrama, S.L. Seneviratne, DENGUE VIRAL INFECTIONS, Indian J. Dermatol. 55 (2010) 68–78. https://doi.org/10.4103/0019-5154.60357.

[6] M. Narayanan, M.A. Aravind, N. Thilothammal, R. Prema, C.S.R. Sargunam, N. Ramamurty, Dengue fever epidemic in Chennai--a study of clinical profile and outcome, Indian Pediatr. 39 (2002) 1027–1033.

[7] P.C.G. Nunes, R.P. Daumas, J.C. Sánchez-Arcila, R.M.R. Nogueira, M.A.P. Horta, F.B. dos Santos, 30 years of fatal dengue cases in Brazil: a review, BMC Public Health. 19 (2019) 329. https://doi.org/10.1186/s12889-019-6641-4.

[8] Boletins epidemiológicos, (n.d.). http://saude.gov.br/boletins-epidemiologicos (accessed October 21, 2018).

[9] H.-R. Chen, Y.-C. Lai, T.-M. Yeh, Dengue virus non-structural protein 1: a pathogenic factor, therapeutic target, and vaccine candidate, J. Biomed. Sci. 25 (2018) 58. https://doi.org/10.1186/s12929-018-0462-0.

[10] A. Figueiredo, N.C.S. Vieira, J.F. dos Santos, B.C. Janegitz, S.M. Aoki, P.P. Junior, R.L. Lovato, M.L. Nogueira, V. Zucolotto, F.E.G. Guimarães, Electrical Detection of Dengue Biomarker Using Egg Yolk Immunoglobulin as the Biological Recognition Element, Sci. Rep. 5 (2015). https://doi.org/10.1038/srep07865.

[11] A.C. Alcalá, R. Hernández-Bravo, F. Medina, D.S. Coll, J.L. Zambrano, R.M. Del Angel, J.E. Ludert, The dengue virus non-structural protein 1 (NS1) is secreted from infected mosquito cells via a non-classical caveolin-1-dependent pathway, J. Gen. Virol. 98 (2017) 2088–2099. https://doi.org/10.1099/jgv.0.000881.

[12] A.C. Alcalá, F. Medina, A. González-Robles, L. Salazar-Villatoro, R.J. Fragoso-Soriano, C. Vásquez, M. Cervantes-Salazar, R.M. Del Angel, J.E. Ludert, The dengue virus non-structural protein 1 (NS1) is secreted efficiently from infected mosquito cells, Virology. 488 (2016) 278–287. https://doi.org/10.1016/j.virol.2015.11.020.

[13] S. Alcon, A. Talarmin, M. Debruyne, A. Falconar, V. Deubel, M. Flamand, Enzyme-Linked Immunosorbent Assay Specific to Dengue Virus Type 1 Nonstructural Protein NS1 Reveals Circulation of the Antigen in the Blood during the Acute Phase of Disease in Patients Experiencing Primary or Secondary Infections, J. Clin. Microbiol. 40 (2002) 376–381. https://doi.org/10.1128/JCM.40.02.376-381.2002.

[14] R.W. Peeling, H. Artsob, J.L. Pelegrino, P. Buchy, M.J. Cardosa, S. Devi, D.A. Enria, J. Farrar, D.J. Gubler, M.G. Guzman, S.B. Halstead, E. Hunsperger, S. Kliks, H.S. Margolis, C.M. Nathanson, V.C. Nguyen, N. Rizzo, S. Vázquez, S. Yoksan, Evaluation of diagnostic tests: dengue, Nat. Rev. Microbiol. 8 (2010) S30-38. https://doi.org/10.1038/nrmicro2459.

[15] O. Parkash, R. Shueb, Diagnosis of Dengue Infection Using Conventional and Biosensor Based Techniques, Viruses. 7 (2015) 5410–5427. https://doi.org/10.3390/v7102877.

[16] K.H. Lee, H. Zeng, Aptamer-Based ELISA Assay for Highly Specific and Sensitive Detection of Zika NS1 Protein, Anal. Chem. 89 (2017) 12743–12748. https://doi.org/10.1021/acs.analchem.7b02862.

[17] I. Palchetti, M. Mascini, Nucleic acid biosensors for environmental pollution monitoring, Analyst. 133 (2008) 846–854. https://doi.org/10.1039/B802920M.

[18] L.K.L. Cheng, P.J. Unrau, Closing the Circle: Replicating RNA with RNA, Cold Spring Harb. Perspect. Biol. 2 (2010) a002204. https://doi.org/10.1101/cshperspect.a002204.

[19] J.C. Burnett, J.J. Rossi, RNA-based therapeutics: current progress and future prospects, Chem. Biol. 19 (2012) 60–71. https://doi.org/10.1016/j.chembiol.2011.12.008.

[20] E.W.M. Ng, D.T. Shima, P. Calias, E.T. Cunningham, D.R. Guyer, A.P. Adamis, Pegaptanib, a targeted anti-VEGF aptamer for ocular vascular disease, Nat. Rev. Drug Discov. 5 (2006) 123–132. https://doi.org/10.1038/nrd1955.

[21] B. Zhou, B. Wang, Pegaptanib for the treatment of age-related macular degeneration, Exp. Eye Res. 83 (2006) 615–619. https://doi.org/10.1016/j.exer.2006.02.010.

[22] S. Shin, I.-H. Kim, W. Kang, J.K. Yang, S.S. Hah, An alternative to Western blot analysis using RNA aptamer-functionalized quantum dots, Bioorg. Med. Chem. Lett. 20 (2010) 3322–3325. https://doi.org/10.1016/j.bmcl.2010.04.040.

[23] S. Lee, K.-M. Song, W. Jeon, H. Jo, Y.-B. Shim, C. Ban, A highly sensitive aptasensor towards Plasmodium lactate dehydrogenase for the diagnosis of malaria, Biosens. Bioelectron. 35 (2012) 291–296. https://doi.org/10.1016/j.bios.2012.03.003.

[24] Y. Wang, D. Xu, H.-Y. Chen, Aptamer-based silver nanosensor for multiple protein detection, Lab. Chip. 12 (2012) 3184–3189. https://doi.org/10.1039/C2LC40322F.

[25] X. Tan, W. Chen, S. Lu, Z. Zhu, T. Chen, G. Zhu, M. You, W. Tan, Molecular Beacon Aptamers for Direct and Universal Quantitation of Recombinant Proteins from Cell Lysates, Anal. Chem. 84 (2012) 8272–8276. https://doi.org/10.1021/ac301764q.

[26] J. Orozco, S. Campuzano, D. Kagan, M. Zhou, W. Gao, J. Wang, Dynamic Isolation and Unloading of Target Proteins by Aptamer-Modified Microtransporters, Anal. Chem. 83 (2011) 7962–7969. https://doi.org/10.1021/ac202029k.

[27] Ö. Kökpinar, J.-G. Walter, Y. Shoham, F. Stahl, T. Scheper, Aptamer-based downstream processing of his-tagged proteins utilizing magnetic beads, Biotechnol. Bioeng. 108 (2011) 2371–2379. https://doi.org/10.1002/bit.23191.

[28] K. Ito, M. Uno, Y. Nakamura, A tripeptide "anticodon" deciphers stop codons in messenger RNA, Nature. 403 (2000) 680–684. https://doi.org/10.1038/35001115.

[29] Y. Huang, S. Zhao, Z.-F. Chen, M. Shi, H. Liang, Amplified fluorescence polarization aptasensors based on structure-switching-triggered nanoparticles enhancement for bioassays, Chem. Commun. 48 (2012) 7480–7482. https://doi.org/10.1039/C2CC33021K.

[30] K. Han, Z. Liang, N. Zhou, Design Strategies for Aptamer-Based Biosensors, Sensors. 10 (2010) 4541–4557. https://doi.org/10.3390/s100504541.

[31] C. Ocaña, M. Pacios, M. Del Valle, A Reusable Impedimetric Aptasensor for Detection of Thrombin Employing a Graphite-Epoxy Composite Electrode, Sensors. 12 (2012) 3037–3048. https://doi.org/10.3390/s120303037.

[32] L. Feng, Y. Chen, J. Ren, X. Qu, A graphene functionalized electrochemical aptasensor for selective label-free detection of cancer cells, Biomaterials. 32 (2011) 2930–2937. https://doi.org/10.1016/j.biomaterials.2011.01.002.

[33] P. Jolly, P. Estrela, M. Ladomery, Oligonucleotide-based systems: DNA, microRNAs, DNA/RNA aptamers, Essays Biochem. 60 (2016) 27–35. https://doi.org/10.1042/EBC20150004.

[34] J.L. Hammond, N. Formisano, P. Estrela, S. Carrara, J. Tkac, Electrochemical biosensors and nanobiosensors, Essays Biochem. 60 (2016) 69–80. https://doi.org/10.1042/EBC20150008.

[35] S.D. Keighley, P. Li, P. Estrela, P. Migliorato, Optimization of DNA immobilization on gold electrodes for label-free detection by electrochemical impedance spectroscopy, Biosens. Bioelectron. 23 (2008) 1291–1297. https://doi.org/10.1016/j.bios.2007.11.012.

[36] P. Zhurauski, S.K. Arya, P. Jolly, C. Tiede, D.C. Tomlinson, P. Ko Ferrigno, P. Estrela, Sensitive and selective Affimer-functionalised interdigitated electrode-based capacitive biosensor for Her4 protein tumour biomarker detection, Biosens. Bioelectron. 108 (2018) 1–8. https://doi.org/10.1016/j.bios.2018.02.041.

[37] M.S. Góes, H. Rahman, J. Ryall, J.J. Davis, P.R. Bueno, A Dielectric Model of Self-Assembled Monolayer Interfaces by Capacitive Spectroscopy, Langmuir. 28 (2012) 9689–9699. https://doi.org/10.1021/la301281y.

[38] T.A. Benites, W.C. Ribeiro, M.S. Góes, A.A.P. Ferreira, P.R. Bueno, EFFECTS OF SURFACE ROUGHNESS ON PROPERTIES OF PASSIVATION OF SELF-ASSEMBLED ORGANIC MONOLAYERS, Quím. Nova. (2014). https://doi.org/10.5935/0100-4042.20140241.

[39] S. Trasatti, O.A. Petrii, Real surface area measurements in electrochemistry, Pure Appl. Chem. 63 (1991) 711–734. https://doi.org/10.1351/pac199163050711.

[40] A.A.P. Ferreira, H. Yamanaka, Microscopia de força atômica aplicada em imunoensaios, Quím. Nova. 29 (2006) 137–142. https://doi.org/10.1590/S0100-40422006000100024.

[41] P.S.P. Herrmann, M.A.P. da Silva, R. Bernardes Fo, A.E. Job, L.A. Colnago, J.E. Frommer, L.H.C. Mattoso, Microscopia de varredura por força: uma ferramenta poderosa no estudo de polímeros, Polímeros. 7 (1997) 51–61. https://doi.org/10.1590/S0104-14281997000400009.

[42] M.A. Edeling, M.S. Diamond, D.H. Fremont, Structural basis of Flavivirus NS1 assembly and antibody recognition, Proc. Natl. Acad. Sci. U. S. A. 111 (2014) 4285–4290. https://doi.org/10.1073/pnas.1322036111.

[43] T.M. Herne, M.J. Tarlov, Characterization of DNA Probes Immobilized on Gold Surfaces, J. Am. Chem. Soc. 119 (1997) 8916–8920. https://doi.org/10.1021/ja9719586.

[44] M. Baghayeri, R. Ansari, M. Nodehi, I. Razavipanah, H. Veisi, Label-free Electrochemical Bisphenol A Aptasensor Based on Designing and Fabrication of a Magnetic Gold Nanocomposite, Electroanalysis. 30 (2018) 2160–2166. https://doi.org/10.1002/elan.201800158.

[45] D.A. Armbruster, T. Pry, Limit of Blank, Limit of Detection and Limit of Quantitation, Clin. Biochem. Rev. 29 (2008) S49–S52.

[46] Genomic analysis and growth characteristic of dengue viruses from Makassar, Indonesia, Infect. Genet. Evol. 32 (2015) 165–177. https://doi.org/10.1016/j.meegid.2015.03.006.

[47] J.M. Lim, J.H. Kim, M.Y. Ryu, C.H. Cho, T.J. Park, J.P. Park, An electrochemical peptide sensor for detection of dengue fever biomarker NS1, Anal. Chim. Acta. 1026 (2018) 109–116. https://doi.org/10.1016/j.aca.2018.04.005.

[48] D. Wasik, A. Mulchandani, M.V. Yates, Salivary Detection of Dengue Virus NS1 Protein with a Label-Free Immunosensor for Early Dengue Diagnosis, Sensors. 18 (2018) 2641. https://doi.org/10.3390/s18082641.

[49] A. Santos, P.R. Bueno, J.J. Davis, A dual marker label free electrochemical assay for Flavivirus dengue diagnosis, Biosens. Bioelectron. 100 (2018) 519–525. https://doi.org/10.1016/j.bios.2017.09.014.

[50] N.T. Darwish, S.D. Sekaran, Y. Alias, S.M. Khor, Immunofluorescence–based biosensor for the determination of dengue virus NS1 in clinical samples, J. Pharm. Biomed. Anal. 149 (2018) 591–602. https://doi.org/10.1016/j.jpba.2017.11.064.

[51] J. Cecchetto, F.C.B. Fernandes, R. Lopes, P.R. Bueno, The capacitive sensing of NS1 Flavivirus biomarker, Biosens. Bioelectron. 87 (2017) 949–956. https://doi.org/10.1016/j.bios.2016.08.097.

[52] J. Cecchetto, F.C. Carvalho, A. Santos, F.C.B. Fernandes, P.R. Bueno, An impedimetric biosensor to test neat serum for dengue diagnosis, Sens. Actuators B Chem. 213 (2015) 150–154. https://doi.org/10.1016/j.snb.2015.02.068.

[53] P.D. Sinawang, V. Rai, R.E. Ionescu, R.S. Marks, Electrochemical lateral flow immunosensor for detection and quantification of dengue NS1 protein, Biosens. Bioelectron. 77 (2016) 400–408. https://doi.org/10.1016/j.bios.2015.09.048.

[54] A.C.M.S. Dias, S.L.R. Gomes-Filho, M.M.S. Silva, R.F. Dutra, A sensor tip based on carbon nanotube-ink printed electrode for the dengue virus NS1 protein, Biosens. Bioelectron. 44 (2013) 216–221. https://doi.org/10.1016/j.bios.2012.12.033.

Highlights

- An electrochemical biosensor for Dengue detection using DNA aptamers.
- Surface characterization through AFM and electrochemical impedance spectroscopy.
- Biosensor identify NS1 serotype 1 and 4 in undiluted human serum in clinical range.
- Platform provided 22 pg/mL as LOD with a linear range from 10 pg to 1 μg/mL.
- Aptasensor was tested with E protein as negative control and show a high selectivity.

Declaration of interests

☒ The authors declare that they have no known competing financial interests or personal relationships that could have appeared to influence the work reported in this paper.

☐The authors declare the following financial interests/personal relationships which may be considered as potential competing interests: